Effect of Underlying Silicon On Performance of Film Bulk Acoustic Resonator (FBAR)

Ajay Kumar [#1], Jitendra Singh [*2]

[#]*Smart Sensors Area, CSIR-Central Electronics Engineering Research Institute*
Pilani, Rajasthan 333031, India
[1]ajayceeri1024@gmail.com
[2]jitendrasingh31@gmail.com

Abstract — **We have realized Barium Strontium Titanate (BST) and Zinc Oxide (ZnO) thin film based Film Bulk Acoustic Resonators (FBAR). The resonator layer stack consists of BST/ZnO bilayer films and used as a piezoelectric layer. The Resonator was fabricated using a standard Silicon Microelectromechanical Systems (MEMS) microfabrication process. Platinum (Pt) was used as electrode material due to its high acoustic impedance (84.74×10^5 g/cm^2-Sec) and its ability to withstand high temperature. Experimentally, it is found that the underlying Silicon has a large effect on the resonance frequency, it was upshifted (1.648 GHz) after complete Si removal. Electromechanical coupling coefficient (K_t^2) of FBAR was also increased (1.183%) after removal of complete Si. Furthermore, spurious modes are removed, which are due to underlying Silicon. Here, the mechanism has been discussed to understand the effect of underlying Silicon on resonance.**

Index Terms — ***ZnO, BST, FBAR, Acoustic, MEMS*** **(key words)**

I. Introduction

Radiofrequency filters and resonators are vital for today's wireless systems. These RF devices are shrinking day by day in size without any compromise in their performances. FBAR devices and filters are fascinating due to the high value of quality factor, high value of operating frequency (up to 20 GHz), good power handling and small size [1]. These BAW resonators and filters are compatible to fabricate on Si-wafer. All these things kindled me to fabricate FBAR. It consists of a piezoelectric layer sandwiched between two metal electrodes. A bulk wave is propagating inside the piezoelectric material by applying a high-frequency signal across the electrode and it resonates at a particular frequency depending on the thickness of the piezoelectric material. The device is fabricated on a Si wafer that is etched from backside by bulk micromachining to release the FBAR membrane. The fundamental resonance is observed when the thickness of the piezoelectric thin film is equivalent to half the wavelength of the Input signal. Condition for mechanical resonance is:

$$f = \frac{(n+1)v_l}{2d} \quad (1)$$

Where f is the resonance frequency, v_l is the acoustic velocity, and d is the thickness of thin film [2]. FBAR exhibits a micromachined air gap to reduce the electromechanical coupling between the substrate and the device. Micromachining is needed to release the FBAR and provide the acoustic isolation between device and the substrate. At resonance, the electrical impedance of the device changes sharply, providing the possibility of designing a frequency selective filter and other switches. Fabrication of FBAR device involves a number of the process step. The bottom and upper electrode are deposited with DC magnetron sputtering of the Ti/Pt material and patterned with a lift-off process. The Piezoelectric layer is deposited with RF magnetron co-sputtering [3].

II. Fabrication

In the recent year with significant progress in FBAR technologies for numerous applications, here we fabricated intrinsically electrically tunable Bi-layer FBAR (Si/SiO_2/Pt/BST/ZnO/Pt). In this we can tune the resonance frequency by application of a DC biased voltage. Our fabrication has six lithography process for the deposition of different thin layer on Si substrate. We used 3 Inch silicon wafer, 100 (P-type) with a thickness around 370 µm. First, by the thermal Oxidation process we grown a SiO_2 (1 µm) layer on both sides of the wafer. SiO_2 layer work as an isolation layer between the device and substrate. Noble gas sputtering system was used for metallization. Upper and bottom electrode both are of Ti/Pt material and they were patterned with standard photolithography process and lift-off process. The thickness of the lower and upper electrode is same 200/2000 Angstrom respectively. There are number of reason to use Pt as electrode: It can withstand high temperature, it has tight-packed grain orientation that avoids the diffusion of the piezoelectric layers and it has a very good value of kt^2 [4]. Reactive magnetron co-sputtering system was used for deposition of a thin layer of BST (300nm) with these parameters: RF power 150W, Ar/O_2 18:2 in SCCM, the temperature during sputtering is maintained at 150°C and sputtered time 120 minutes and post annealed at 800°C [5]. BST thin film etched with Buffer oxy etchant with etching rate of 2.727 nm/second [6]. Reactive co-sputtering was used for deposition of a thin layer of piezoelectric material

(ZnO) with these parameters: RF power 400W, constant chamber pressure of 20 mTorr (Ar/O_2 20/30 SCCM) and sputtered time was 240 minutes and patterned by 0.25% hydrochloric solution [7].

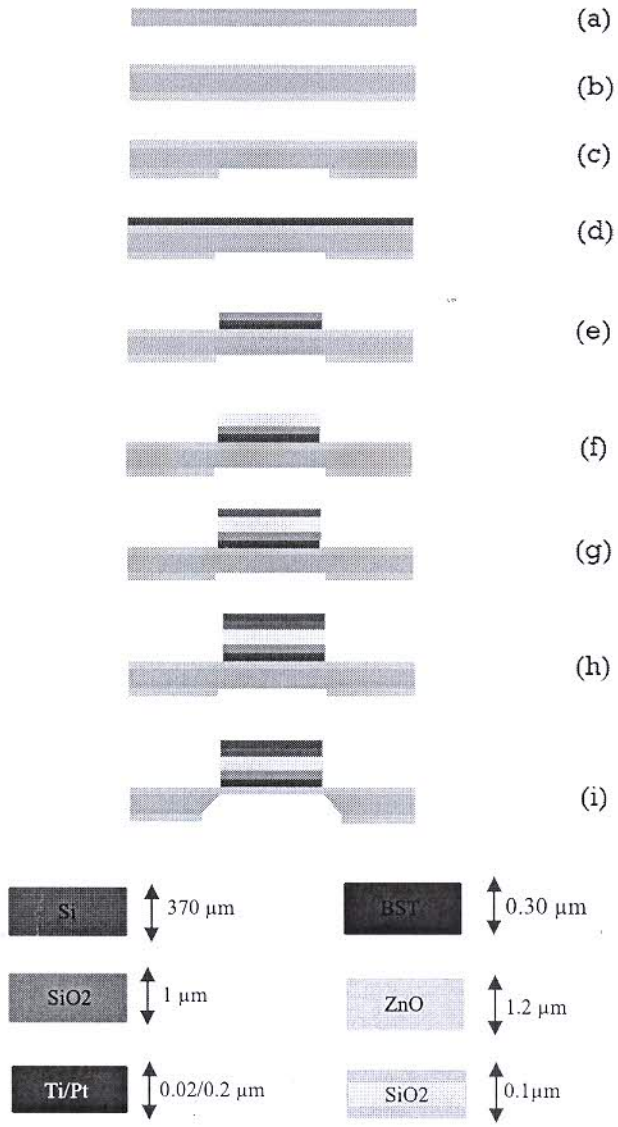

Fig. 1. Tunable FBAR fabrication process steps represent by schematic sketch

We use ZnO as a piezoelectric layer because it has a high value of piezoelectric coefficient (d_{33}) and piezoelectric coupling coefficient (k^2_{eff}) [8]. ZnO has a high value of quality factor and stability despite of low insertion losses [9]. In FBAR fabrication process to provide isolation between the lower stack and upper electrode we deposited a thin layer of SiO_2 (100nm) by Plasma-enhanced chemical vapor deposition (PECVD) at these parameters: RF power 80W in the presence of Ar, N_2O, N_2 and SiH_4. Fig.1. show the schematic sketch for fabrication of tunable thin-film bulk acoustic wave resonator. We etched the silicon from the backside of the wafer by bulk micromachining with Tetramethyl ammonium hydroxide (TMAH) [10] and DRIE. We used a wafer holder that is made of PTFE (Poly tetra fluoro-ethylene), It is a thermoplastic polymer which is white solid at room temperature, with a density of about 2200 Kg/m^3.According to chemours, it's melting point is 600K (327°C or 620°F). The use of PTFE is a function of its resistance to chemical attack, un-reactivity (above 500 K), low friction, non-stick properties and high electrical resistance. We have a PTFE wafer holder that protects one-side of the wafer from etching in TMAH solution. The wafer holder can place easily with a reflux condenser setup in the beaker and a mercury thermometer is used to measure the temperature of the solution. We experimentally optimized that the TMAH (25% concentrated) etching rate with 100 orientation is maintained at 0.5 µm/minutes by keeping constant temperature 80°C of solution. We etched silicon with TMAH approximately 320 - 350 µm [7] and then DRIE (Deep Reactive-ion etching). In FBAR fabrication, first the devices are fabricated on one side of the wafer with a different thin layer and then etched the wafer from backside to form micro-cavity under FBAR Structure.

III. Result and Discussion

Thin-film stack (Pt/BST/ZnO) is analysed by X-ray diffraction (XRD) equipped with Cu source. The detector was scanned in 2θ range from 10° to 80° with a scan rate of 3°/min. Diffraction peak of Pt was observed with 111 and 110 orientation tend to align parallel to the substrate. Usually c-axis oriented ZnO film have polar phase and high piezoelectric value. Diffraction peaks of ZnO have intense sharp peak with orientation (0002) at 34.382° and (103) at 62.64° [11]. BST was deposited and post annealed at 800°C to obtained good crystallinity and we obtained high intense peak at 45° with (200) orientation [12].

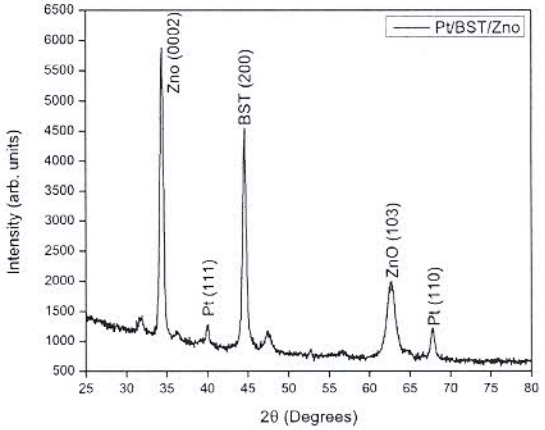

Fig. 2. X-ray diffraction of stack Pt/BST/ZnO

The sharp peaks for BST and ZnO confirmed these films have very good crystallinity. Structural analysis of fabricated Single port BST/ZnO based FBAR is done with Scanning electron microscopy (SEM) (Fig.3) and its piezoelectric active area is 9636 μm^2 with approx. square-shaped. Black shadow region around the active area is the impression of SiO_2 after underlying silicon etched completely. The Spacing between resonance and anti-resonance frequency, the electromechanical coupling constant [13] and effective coupling constant are calculated from S11 impedance vs frequency plot with following.

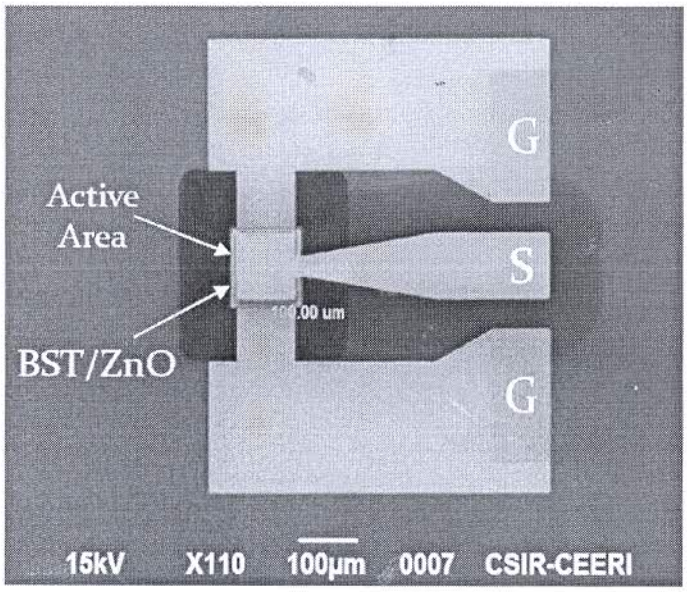

Fig. 3. Scanning electron microscopy of Resonators with Active area

Vector network analyzer (VNA) and probe station is used to measure the RF characteristics of resonators. We measured S11, impedance and their phase characteristics. It was observed that by etching of silicon we can increase the resonance frequency, Bandwidth and $\%Kt^2$. The main reason to increase in resonance frequency due to the backside etching of silicon is that RF losses are diminished by reducing the electrical coupling between FBAR and substrate.

We experimentally calculated the effect of the underlying silicon on performance of the FBAR. We etched silicon in three-step, 1st step Si etched around 288 µm, in 2nd step etched around 335 µm and in 3rd it was around 370 and characterize with VNA to obtained series and parallel resonance frequency, electromechanical coupling coefficient and effective coupling coefficient.

$$k_t^2 = \frac{\pi^2}{4}\frac{f_p}{f_s}\frac{f_p^2 - f_s^2}{f_p^2} \quad (2)$$

$$k_{eff}^2 = \frac{f_p^2 - f_s^2}{f_p^2} \quad (3)$$

A typical comparison between the resonance frequency of square shape resonator with the effect of underlying layer has shown in the following table:

TABLE 1. Upward shift in resonance frequency with effect of underlying silicon

Resonator	f_s (GHz)	f_p (GHz)	$\%Kt^2$	$\%K^2_{eff}$
Si left 80 µm	0.965	0.967	0.496	0.402
Si left 35µm	0.98	0.983	0.751	0.609
Si fully etched	1.648	1.655	1.183	0.964

After each step, we measured the thickness of Si from DEKTAK- 6M Surface profiler. We etched all-silicon under FBAR structure and only SiO_2 layer left at last under device or we can say that FBAR on SiO_2 layer only. As we observed in FIG. 4 that by removing underlying silicon, one fundamental mode of resonance is observed. The Acoustic wave that propagates in FBAR are thickness excited wave (propagate parallel to the electric field) and lateral excited wave (propagate perpendicular to the electric field). Because of the orientation of the deposited piezoelectric layer the TE mode is excited [13] and the lateral wave is undesirable and generates spurious mode that may degrade the performance of FBAR. These spurious modes are basically due to laterally leakage wave and acoustic wave leakage in Si substrate. Spurious mode generated by the lateral wave is minimized by technique apodization and lateral resonator edge design. There should be large acoustic wave mismatch between FBAR electrode and surrounding of FBAR. So we have etched the Si beneath the lower electrode to create a device with high quality factor and bandwidth [14]. The removal of underlying silicon not only reduces the unwanted mode but also increase the resonance frequency of FBAR.

Due to mass loading effect there is a change in resonant frequency of FBAR or we can say that we are reducing the anchor loss of FBAR by etching all of the silicon and there will be increase in FBAR performance due to less losses [15]. We achieved a shift in resonance frequency from 0.965 GHz to 1.648 and effective electromechanical coupling factor increase from 0.404 to 0.964 as mentioned in table1. Series Resonance

frequency increase by 70.77% due to etched all-silicon under lower electrode.

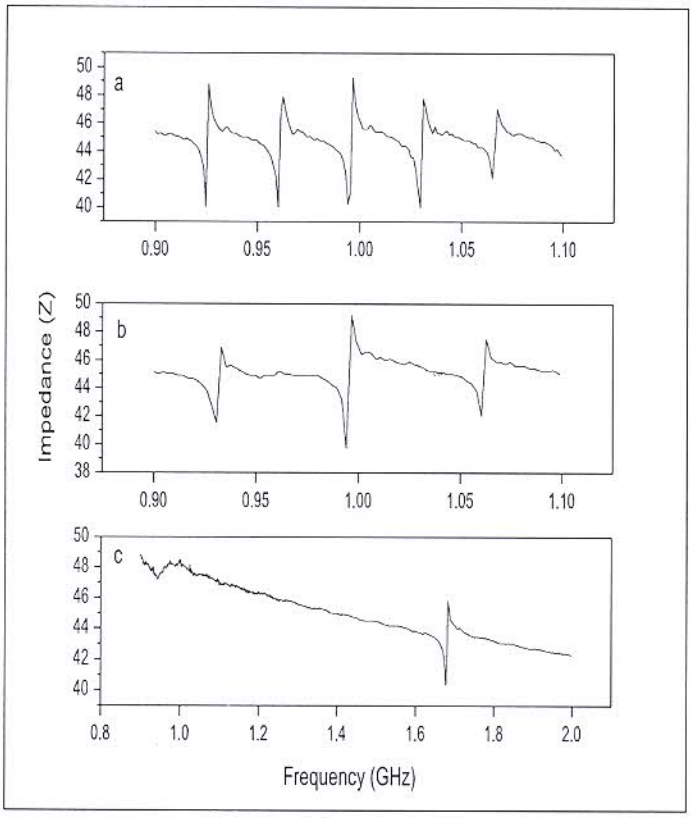

Fig. 4. Effect of underlying silicon on FBAR, S11 Impedance plotted with frequency, (a) Si left 80 μm, (b) Si left 35 μm (c) Fully etched underlying Si

IV. Conclusions

BST/ZnO based intrinsically tunable resonator has fabricated for frequency tuning. In this, we calculated the effect of underlying silicon on the performance of resonator. We calculated S11 impedance vs frequency at the different thickness of underlying silicon with VNA. We experimentally found an increase in resonance frequency from 0.965 GHz to 1.648 GHz when we etched underlying all-silicon from FBAR stack and spurious or unwanted mode are reduced, fully Si-etched FBAR has only one fundamental mode. Parameter related to resonance frequency such as electromechanical coupling coefficient and effective electromechanical coupling coefficient also increased.

Acknowledgement

The authors are thankful to the fabrication team of "Smart Sensor Area" in **CSIR-CEERI Pilani, Rajasthan**. This research work was financially sponsored by the science and Engineering Research Board, a statuary body of Department of Science and Technology (DST), Government of India (SERB-DST Grant No. EMR/2016/006279).

References

[1] Dong, S. R., Bian, X. L., Jin, H., Hu, N. N., Zhou, J., Wong, H., & Deen, M. J. (2013). Electrically tunable film bulk acoustic resonator based on Au/ZnO/Al structure. *Applied Physics Letters*, *103*(6), 062904.

[2] G. Hashimoto, K. Y. (2009). RF bulk acoustic wave filters for communications. Artech House.

[3] Singh, J., Kumar, A., Das, S., & Kothari, P. (2018, November). Tunable Film Bulk Acoustic Wave Resonator Based on Magnetostrictive Fe 65 Co 35 Thin Films. In *2018 Asia-Pacific Microwave Conference (APMC)* (pp. 800-802). IEEE.

[4] Okamoto, S., Watanabe, T., Akiyama, K., Kaneko, S., Funakubo, H., & Horita, S. (2005). Epitaxial Pt films with different orientations grown on (100) Si substrates by RF magnetron sputtering. *Japanese journal of applied physics*, *44*(7R), 5102.

[5] Barala, S. S., Singh, J., Ranwa, S., & Kumar, M. (2015). Radiation Induced Response of ${\rm Ba} _ {0.5}{\rm Sr} _ {0.5}{\rm TiO} _3 S Based Tunable Capacitors Under Gamma Irradiation. *IEEE Transactions on Nuclear Science*, *62*(4), 1873-1878.

[6] Zhang, T., Huang, H., & Chen, R. (2010). Wet chemical etching process of BST thin films for pyroelectric infrared detectors. *Ferroelectrics*, *410*(1), 137-144.

[7] Joshi, P., Singh, J., Sharma, R., Jain, V. K., & Akhtar, J. (2018). A facile approach to fabricate ZnO thin film based micro-cantilevers. Microelectronic Engineering, 187, 50-57.

[8] Denishev, K. (2016, October). Some metal oxides and their applications for creation of Microsystems (MEMS) and Energy Harvesting Devices (EHD). In *Journal of Physics: Conference Series* (Vol. 764, No. 1, p. 012003). IOP Publishing.

[9] Su, Q. X., Kirby, P., Komuro, E., Imura, M., Zhang, Q., & Whatmore, R. (2001). Thin-film bulk acoustic resonators and filters using ZnO and lead-zirconium-titanate thin films. *IEEE Transactions on Microwave Theory and Techniques*, *49*(4), 769-778.

[10] Lucklum, R., & Hauptmann, P. (2006). Acoustic microsensors—the challenge behind microgravimetry. *Analytical and bioanalytical chemistry*, *384*(3), 667-682.

[11] Fang, Te-Hua, et al. "Effect of annealing on the structural and mechanical properties of Ba0. 7Sr0. 3TiO3 thin films." Materials Science and Engineering: A 426.1-2 (2006): 157-161.

[12] Chen, Q., & Wang, Q. M. (2005). The effective electromechanical coupling coefficient of piezoelectric thin-film resonators. *Applied Physics Letters*, *86*(2), 022904.

[13] Wang, Ye, Seungbae Lee, and Harmeet Bhugra. "Thin-film bulk acoustic resonators having perforated resonator body supports that enhance quality factor." U.S. Patent No. 8,106,724. 31 Jan. 2012.

[14] Aigner, Robert. "High performance RF-filters suitable for above IC integration: film bulk-acoustic-resonators (FBAR) on silicon." *Proceedings of the IEEE 2003 Custom Integrated Circuits Conference, 2003.*. IEEE, 2003.

[15] Nguyen, C. C., Katehi, L. P., & Rebeiz, G. M. (1998). Micromachined devices for wireless communications. *Proceedings of the IEEE*, *86*(8), 1756-1768.